

# Fast estimation of polarization power spectra using correlation functions

Gayoung Chon,<sup>1\*</sup> Anthony Challinor,<sup>1</sup> Simon Prunet,<sup>2</sup> Eric Hivon,<sup>3</sup> and István Szapudi<sup>4</sup>

<sup>1</sup>*Astrophysics Group, Cavendish Laboratory, Madingley Road, Cambridge CB3 0HE, U.K.*

<sup>2</sup>*Institut d'Astrophysique de Paris, 98bis, Boulevard Arago, 75014 Paris, France*

<sup>3</sup>*Infrared Processing and Analysis Center, Caltech, 770 South Wilson Avenue, Pasadena, CA 91125, U.S.A.*

<sup>4</sup>*Institute for Astronomy, University of Hawaii, 2680 Woodlawn Dr, Honolulu, HI 96822, U.S.A.*

24 October 2018

## ABSTRACT

We present a fast method for estimating the cosmic microwave background polarization power spectra using unbiased estimates of heuristically-weighted correlation functions. This extends the  $O(N_{\text{pix}}^{3/2})$  method of Szapudi et al. (2001) to polarized data. If the sky coverage allows the correlation functions to be estimated over the full range of angular separations, they can be inverted directly with integral transforms and clean separation of the electric ( $E$ ) and magnetic ( $B$ ) modes of polarization is obtained exactly in the mean. We assess the level of  $E$ - $B$  mixing that arises from apodized integral transforms when the correlation function can only be estimated for a subset of angular scales, and show that it is significant for small-area observations. We introduce new estimators to deal with this case on the spherical sky that preserve  $E$ - $B$  separation; their construction requires an additional integration of the correlation functions but the computational cost is negligible. We illustrate our methods with application to a large-area survey with parameters similar to *Planck*, and the small-area Background Imaging of Cosmic Extragalactic Polarization experiment. In both cases we show that the errors on the recovered power spectra are close to theoretical expectations.

**Key words:** cosmic microwave background – methods: analytical: – methods: numerical.

## 1 INTRODUCTION

With the recent detection of polarization in the cosmic microwave background (CMB) by the Degree Angular Scale Interferometer (DASI; Kovac et al. 2002), and the detection of the temperature-polarization cross correlation by the *Wilkinson Microwave Anisotropy Probe (WMAP)*<sup>1</sup> (Kogut et al. 2003), the immediate goal for upcoming polarization experiments is to map accurately the polarization power spectra over a wide range of angular scales. CMB polarization is generated at last scattering from the local quadrupole moment of the photon total intensity. The expected r.m.s. polarization is  $\sim 6.4 \mu\text{K}$ , peaking around an angular scale of  $\sim 10$  arcmin (the angle subtended by the width of the last scattering surface), making mapping a challenging prospect. Further scattering once the Universe reionizes tends to destroy polarization on scales that are then sub-Hubble, but

generates additional large-angle polarization (Zaldarriaga 1997). The potential cosmological returns from polarization observations are high. Current polarization data (Kovac et al. 2002; Kogut et al. 2003) already allows a stringent test to be made of the paradigm for structure formation from initially super-Hubble, passive, adiabatic fluctuations. Furthermore, the detection by *WMAP* of large-scale power in the temperature-polarization cross power spectrum has provided new constraints on the reionization process, and helped lift major degeneracies that affect the determination of cosmological parameters from the CMB temperature anisotropies. (In particular, the degeneracies between reionization optical depth and the scalar spectral index and gravitational wave amplitude.) Potential returns from future, more precise, observations include (i) detection of the clean signature of a stochastic background of gravitational waves (Seljak & Zaldarriaga 1997; Kamionkowski, Kosowsky & Stebbins 1997) and hence fine selection between inflation models (Kinney 1998); and (ii) evidence for weak gravitational lensing through the distortion of CMB polariza-

\* E-mail: gchon@mrao.cam.ac.uk

<sup>1</sup> <http://map.gsfc.nasa.gov/>

tion on small scales (Zaldarriaga & Seljak 1998; Benabed, Bernardeau & van Waerbeke 2001). Estimating the polarization power spectra is an important intermediate step in achieving these science goals. This paper addresses that problem, presenting a fast, robust method for estimating the power spectra from large datasets in the presence of real-world complications, such as incomplete sky coverage and inhomogeneous noise.

The accurate analysis of CMB data places strong demands on the statistical methods employed. Even for total intensity data, which is simpler than polarization, the extraction of the power spectrum from upcoming megapixel datasets with standard maximum-likelihood methods (e.g. Bond, Jaffe & Knox 1998) is beyond the range of any supercomputer. [The operations count scales as the number of pixels cubed,  $N_{\text{pix}}^3$ , while the storage requirements are  $O(N_{\text{pix}}^2)$ .] In the search for fast alternatives to brute-force maximum-likelihood power spectrum estimation, two broad approaches have emerged. In the first, experiment-specific symmetries are exploited to make the brute-force analysis tractable, or, if the symmetries are only approximate, to pre-condition an iterative solution to the likelihood maximisation. An example of the former is the ingenious “ring-torus” method of Wandelt & Hansen (2003), while the latter was pioneered by Oh, Spergel & Hinshaw (1999) during the development of the pipeline for the *WMAP* satellite. The second class of methods sacrifice optimality in favour of speed by adopting a more heuristic weighting of the data (such as inverse weighting with the noise variance). An estimate of the underlying power spectrum is then obtained from the raw, rotationally-invariant power spectrum of the weighted map (the pseudo- $C_l$ s; Wandelt, Hivon & Górski 2001) either by a direct linear inversion (Szapudi, Prunet & Colombi 2001; Hivon et al. 2002) or with likelihood methods (Wandelt et al. 2001; Hansen, Górski & Hivon 2002). The linear inversion, which yields estimators quadratic in the data, can be performed directly in harmonic space (Hivon et al. 2002), or, more simply, by first transforming to real space (i.e. by constructing the correlation function) and then recovering the power spectrum with a (suitably apodized) integral transform (Szapudi et al. 2001). The estimation of polarization power spectra is less well explored than for total intensity, although all of the above methods can, in principle, be extended to handle polarization. To date, only brute-force maximum likelihood (Kovac et al. 2002, Munshi et al. in preparation), minimum-variance quadratic estimators (Tegmark & de Oliveira-Costa 2002), pseudo- $C_l$  methods with statistical (Hansen & Górski 2003) or direct inversion (Kogut et al. 2003) in harmonic space, and real-space correlation function methods (Sbarra et al. 2003) have been demonstrated on polarized data. Of these, only the pseudo- $C_l$  methods are fast enough to apply many times (e.g. in Monte-Carlo simulations) to mega-pixel maps. In this paper we extend the fast correlation-function approach of Szapudi et al. (2001) to polarized data.

A new problem that arises when analysing polarized data, that is absent for total intensity, is the decomposition of the polarized field into its electric ( $E$ ; sometimes denoted gradient) and magnetic ( $B$ ; alternatively curl) components. The scientific importance of this decomposition is that primordial magnetic polarization is not generated by density perturbations, and so in standard models is sourced

only by gravitational waves (Seljak & Zaldarriaga 1997; Kamionkowski et al. 1997). However, with incomplete sky coverage, separating the polarization field into electric and magnetic components is no longer straightforward. Exquisite monitoring of leakage between  $E$  and  $B$  in analysis pipelines will be required if primordial  $B$  polarization is to be detected down to the fundamental confusion limit set by cosmic shear (Kesden, Cooray & Kamionkowski 2002). The question of performing the  $E$ - $B$  separation on an incomplete sky has received considerable attention recently (Zaldarriaga 2001; Lewis, Challinor & Turok 2002; Bunn 2002; Chiueh & Ma 2002; Bunn et al. 2003). Methods are now available for extracting pure measures of the  $E$  and  $B$  fields which can then be used for subsequent power spectrum estimation. An alternative approach is to perform a joint (i.e.  $E$  and  $B$ ) power spectrum analysis of the original polarization data, removing the need for an additional stage in the analysis pipeline and the non-optimality that this may introduce. The efficacy of maximum-likelihood methods for performing the  $E$ - $B$  separation is explored by Munshi et al. (in preparation). However, the computational demands of likelihood methods, and the difficulty in monitoring  $E$ - $B$  leakage in a non-linear analysis, motivates the development of fast, unbiased methods. The correlation-function based approach we develop here, motivated by Crittenden et al. (2002), has a significant feature in that, with a little post-processing of the correlation functions, leakage between  $E$  and  $B$  can be eliminated in the mean, even for observations covering only a small part of the sky. The separation is exact in the mean.

The outline of this paper is as follows. In Sec. 2 we review the polarization functions on the sphere and their relation with the power spectra. Section 3 presents a fast,  $O(N_{\text{pix}}^{3/2})$  method for computing unbiased estimates of the correlation functions allowing for heuristic weighting of the data, and describes power spectrum recovery for large-area surveys where the correlation function can be estimated for the full range of angular separations. We illustrate our methods by applying them to a survey mission with similar parameters to those for *Planck*<sup>2</sup>. In Sec. 4 we provide a careful analysis of the effect of incomplete coverage of the correlation functions on the direct extraction of the power spectra with apodized integral transforms. By constructing the relevant window functions for small-area observations we show that leakage from  $E$  to  $B$  can be a significant problem. We remedy this deficiency of the method in Sec. 5, where we construct functions from integrals of the original correlation functions that contain signal contributions from only  $E$  or  $B$  in the mean. These functions can be safely inverted with apodized integral transforms to obtain properly separated estimates of the  $E$  and  $B$  power spectra. We apply this new estimator to a model of the Background Imaging of Cosmic Extragalactic Polarization experiment (BICEP)<sup>3</sup> experiment, and show that it produces error bars close to the theoretical expectations. Our conclusions are given in Sec. 6, and the Appendix contains some technical results on the analytic normalisation of the correlation functions estimators for uniform weighting on azimuthally-symmetric patches.

<sup>2</sup> <http://sci.esa.int/home/planck/>

<sup>3</sup> <http://bicep.caltech.edu>

Throughout this paper we illustrate our results with a flat,  $\Lambda$ CDM model with concordance parameters  $\Omega_b h^2 = 0.022$ ,  $\Omega_c h^2 = 0.12$ ,  $\Omega_\Lambda = 0.7$  giving the Hubble constant  $h = 0.69$ . The primordial scalar curvature and tensor spectra are scale-invariant and have ratio  $r = 0.31$  (making the ratio of tensor to scalar power in temperature anisotropies  $r_{10} = 0.16$  at  $l = 10$ )<sup>4</sup>. We ignore the effects of weak gravitational lensing. We consider two models for the ionization history: no reionization and full reionization at redshift  $z_{\text{re}} = 6$ . Note that had we adopted a model with earlier reionization, e.g.  $z_{\text{re}} \sim 15$  as favoured by *WMAP* data (Kogut et al. 2003), the problem of  $E$ - $B$  mixing described in Section 4 would have been further exacerbated by the additional large-scale  $E$  power.

## 2 POLARIZATION CORRELATION FUNCTIONS ON THE SPHERE

Stokes parameters  $Q(\hat{\mathbf{n}})$  and  $U(\hat{\mathbf{n}})$  are defined for a line of sight  $\hat{\mathbf{n}}$  with the local  $x$ -axis generated by  $\hat{\theta}$  and the local  $y$ -axis by  $-\hat{\phi}$ . Here  $\hat{\theta}$  and  $\hat{\phi}$  are the basis vectors of a spherical-polar coordinate system. A right-handed basis is completed by the addition of the radiation propagation direction  $-\hat{\mathbf{n}}$ . The polarization  $P \equiv Q + iU$  is spin  $-2$  (Newman & Penrose 1966) and can be expanded in spin- $\pm 2$  harmonics as (Seljak & Zaldarriaga 1997)

$$(Q \pm iU)(\hat{\mathbf{n}}) = \sum_{lm} (E_{lm} \mp iB_{lm})_{\mp 2} Y_{lm}(\hat{\mathbf{n}}). \quad (1)$$

Reality of  $Q$  and  $U$  demands  $E_{lm}^* = (-1)^m E_{l-m}$  with an equivalent result for  $B_{lm}$ . Under parity transformations,  $(Q \pm iU)(\hat{\mathbf{n}}) \rightarrow (Q \mp iU)(-\hat{\mathbf{n}})$  so that  $E_{lm}$  has parity  $(-1)^l$  (electric), but  $B_{lm}$  has parity  $(-1)^{l+1}$  (magnetic). The temperature is a scalar field and so can be expanded in spherical harmonics with multipoles  $T_{lm}$ . In an isotropic- and parity-invariant ensemble the non-vanishing elements of the polarization covariance structure are

$$\langle E_{lm} E_{l'm'}^* \rangle = \delta_{ll'} \delta_{mm'} C_l^E, \quad (2)$$

$$\langle B_{lm} B_{l'm'}^* \rangle = \delta_{ll'} \delta_{mm'} C_l^B, \quad (3)$$

$$\langle E_{lm} T_{l'm'}^* \rangle = \delta_{ll'} \delta_{mm'} C_l^{TE}. \quad (4)$$

If the direction  $\hat{\mathbf{n}}_1$  corresponds to angular coordinates  $(\theta_1, \phi_1)$ , and similarly for  $\hat{\mathbf{n}}_2$ , then the  $\text{SO}(3)$  composition

$$D^{-1}(\phi_1, \theta_1, 0) D(\phi_2, \theta_2, 0) = D(\alpha, \beta, -\gamma) \quad (5)$$

determines  $\beta$  ( $0 \leq \beta \leq \pi$ ), the angle between  $\hat{\mathbf{n}}_1$  and  $\hat{\mathbf{n}}_2$ ,  $\alpha$ , the angle required to rotate  $\hat{\theta}(\hat{\mathbf{n}}_1)$  in a right-handed sense about  $\hat{\mathbf{n}}_1$  onto the tangent (at  $\hat{\mathbf{n}}_1$ ) to the geodesic connecting  $\hat{\mathbf{n}}_1$  and  $\hat{\mathbf{n}}_2$ , and  $\gamma$ , defined in the same manner as  $\alpha$  but at  $\hat{\mathbf{n}}_2$ . Making use of the relation between the Wigner- $D$  matrices (e.g. Varshalovich et al. 1988) and the spin-weight spherical harmonics,

$$D_{-ms}^l(\phi, \theta, 0) = (-1)^m \sqrt{\frac{4\pi}{2l+1}} s Y_{lm}(\hat{\mathbf{n}}), \quad (6)$$

we obtain the following representation of equation (5):

<sup>4</sup> We define  $r$  as the ratio of the amplitudes  $A_S$  and  $A_T$  of the primordial curvature and tensor power spectra, following the conventions of Martin & Schwarz (2000).

$$D_{ss'}^l(\alpha, \beta, -\gamma) = \sum_m \frac{4\pi}{2l+1} s Y_{lm}^*(\hat{\mathbf{n}}_1)_{s'} Y_{lm}(\hat{\mathbf{n}}_2). \quad (7)$$

With this result, the two-point correlation functions for linear polarization evaluate to (Ng & Liu 1999)

$$\langle \bar{P}(\hat{\mathbf{n}}_1) \bar{P}(\hat{\mathbf{n}}_2) \rangle = \sum_l \frac{2l+1}{4\pi} (C_l^E - C_l^B) d_{2-2}^l(\beta), \quad (8)$$

$$\langle \bar{P}^*(\hat{\mathbf{n}}_1) \bar{P}(\hat{\mathbf{n}}_2) \rangle = \sum_l \frac{2l+1}{4\pi} (C_l^E + C_l^B) d_{22}^l(\beta), \quad (9)$$

$$\langle T(\hat{\mathbf{n}}_1) \bar{P}(\hat{\mathbf{n}}_2) \rangle = \sum_l \frac{2l+1}{4\pi} C_l^{TE} d_{20}^l(\beta), \quad (10)$$

where  $d_{mn}^l$  are the reduced  $D$ -matrices. Note that  $\langle T(\hat{\mathbf{n}}_1) \bar{P}(\hat{\mathbf{n}}_2) \rangle = \langle \bar{P}(\hat{\mathbf{n}}_1) T(\hat{\mathbf{n}}_2) \rangle$ . The quantities

$$\bar{P}(\hat{\mathbf{n}}_1) \equiv e^{2i\alpha} P(\hat{\mathbf{n}}_1), \quad (11)$$

$$\bar{P}(\hat{\mathbf{n}}_2) \equiv e^{2i\gamma} P(\hat{\mathbf{n}}_2), \quad (12)$$

are the polarizations defined on local bases with the  $x$ -direction along the geodesic between  $\hat{\mathbf{n}}_1$  and  $\hat{\mathbf{n}}_2$ . With these rotations, the correlation functions depend only on the angle  $\beta$  between the two points. Note that  $\langle \bar{P}^*(\hat{\mathbf{n}}_1) \bar{P}(\hat{\mathbf{n}}_2) \rangle$  is real, which follows from statistical isotropy, while  $\langle \bar{P}(\hat{\mathbf{n}}_1) \bar{P}(\hat{\mathbf{n}}_2) \rangle$  and  $\langle T(\hat{\mathbf{n}}_1) \bar{P}(\hat{\mathbf{n}}_2) \rangle$  are only real if the universe is parity-invariant in the mean. In the presence of parity violations,

$$\langle \bar{P}(\hat{\mathbf{n}}_1) \bar{P}(\hat{\mathbf{n}}_2) \rangle = \sum_l \frac{2l+1}{4\pi} [(C_l^E - C_l^B - 2iC_l^{EB}) \times d_{2-2}^l(\beta)], \quad (13)$$

$$\langle T(\hat{\mathbf{n}}_1) \bar{P}(\hat{\mathbf{n}}_2) \rangle = \sum_l \frac{2l+1}{4\pi} (C_l^{TE} - iC_l^{TB}) d_{20}^l(\beta), \quad (14)$$

where

$$\langle E_{lm} B_{l'm'}^* \rangle = \delta_{ll'} \delta_{mm'} C_l^{EB}, \quad \langle T_{lm} B_{l'm'}^* \rangle = \delta_{ll'} \delta_{mm'} C_l^{TB}. \quad (15)$$

The correlation functions of the (rotated) Stokes parameters can be found directly from those for  $\bar{P}$ . Defining

$$\xi_-(\beta) \equiv \langle \bar{P}(\hat{\mathbf{n}}_1) \bar{P}(\hat{\mathbf{n}}_2) \rangle, \quad (16)$$

$$\xi_+(\beta) \equiv \langle \bar{P}^*(\hat{\mathbf{n}}_1) \bar{P}(\hat{\mathbf{n}}_2) \rangle, \quad (17)$$

$$\xi_X(\beta) \equiv \langle T(\hat{\mathbf{n}}_1) \bar{P}(\hat{\mathbf{n}}_2) \rangle, \quad (18)$$

we have

$$\langle \bar{Q}(\hat{\mathbf{n}}_1) \bar{Q}(\hat{\mathbf{n}}_2) \rangle = \frac{1}{2} [\xi_+(\beta) + \Re \xi_-(\beta)], \quad (19)$$

$$\langle \bar{U}(\hat{\mathbf{n}}_1) \bar{U}(\hat{\mathbf{n}}_2) \rangle = \frac{1}{2} [\xi_+(\beta) - \Re \xi_-(\beta)], \quad (20)$$

$$\langle \bar{Q}(\hat{\mathbf{n}}_1) \bar{U}(\hat{\mathbf{n}}_2) \rangle = \frac{1}{2} \Im \xi_-(\beta), \quad (21)$$

$$\langle T(\hat{\mathbf{n}}_1) \bar{Q}(\hat{\mathbf{n}}_2) \rangle = \Re \xi_X(\beta), \quad (22)$$

$$\langle T(\hat{\mathbf{n}}_1) \bar{U}(\hat{\mathbf{n}}_2) \rangle = \Im \xi_X(\beta). \quad (23)$$

In Fig. 1 we plot the correlation functions  $\xi_{\pm}(\beta)$  and  $\xi_X(\beta)$  for the cosmological models described in Sec. 1. The damping of the polarization power on linear scales that are sub-Hubble at the epoch of reionization (in this case at  $z = 6$ ) is just discernible in the correlation functions in Fig. 1. The additional large-scale power due to reionization makes a negligible contribution to the correlation functions for the angular range we have plotted.

We can invert equations (9), (13) and (14) using the orthogonality of the  $d_{mn}^l$ ,

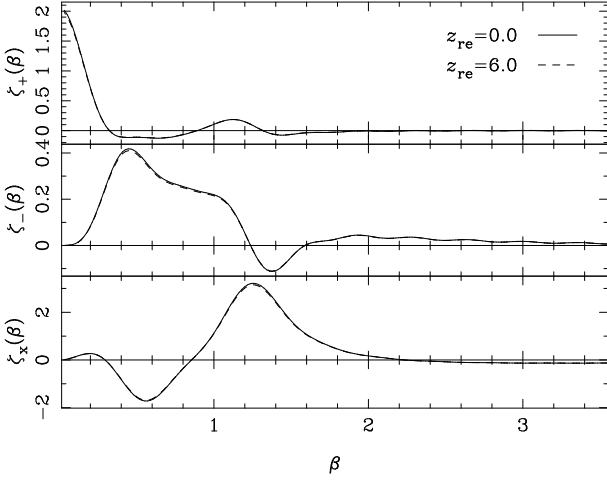


**Figure 1.** The correlation functions  $\xi_+(\beta)$  (top panel),  $\xi_-(\beta)$  (middle), and  $\xi_X(\beta)$  (bottom). The cosmological model is as described in Sec. 1; the solid lines are for no reionization, while the dashed have complete reionization with  $z_{\text{re}} = 6$ . The angle  $\beta$  is in degrees.

$$\int_{-1}^1 d_{mm'}^l(\beta) d_{mm'}^{l'}(\beta) d \cos \beta = \frac{2}{2l+1} \delta_{ll'}, \quad (24)$$

to determine the power spectra from the correlation functions:

$$C_l^E - C_l^B - 2iC_l^{EB} = 2\pi \int_{-1}^1 \xi_-(\beta) d_{2-2}^l(\beta) d \cos \beta, \quad (25)$$

$$C_l^E + C_l^B = 2\pi \int_{-1}^1 \xi_+(\beta) d_{22}^l(\beta) d \cos \beta, \quad (26)$$

$$C_l^{TE} + iC_l^{TB} = 2\pi \int_{-1}^1 \xi_X(\beta) d_{20}^l(\beta) d \cos \beta. \quad (27)$$

Since those reduced  $D$ -matrices that appear in these equations are polynomials in  $\cos \beta$  for, the integrals can be performed essentially exactly for band-limited data by Gauss-Legendre quadrature.

### 3 FAST CORRELATION FUNCTION ESTIMATORS

If we had available unbiased estimates of the various correlation functions for all angles  $0 \leq \beta \leq \pi$ , we could obtain unbiased estimates of the power spectra by performing the inversions in equations (25)–(27). Direct evaluation of the correlation functions (e.g. Sbarra et al. 2003) requires  $O(N_{\text{pix}}^2)$  evaluations and is complicated by the need to perform a rotation to the appropriate basis for each pair of points. Here we consider an  $O(N_{\text{pix}}^{3/2})$  method based on fast spherical transforms. This method generalises that of Szapudi et al. (2001) to polarization fields.

We consider an arbitrary weighting of the noisy polarization field  $P(\hat{\mathbf{n}})$  and the noisy temperature field  $T(\hat{\mathbf{n}})$  with some weight functions  $w_P(\hat{\mathbf{n}})$  and  $w_T(\hat{\mathbf{n}})$  respectively. The weight is zero for those pixels in regions that are either not observed or are removed from the map due to foreground contamination. In this paper we only consider real weighting of the polarization field, thus preserving the direction of

polarization at any point; relaxing this condition is straightforward if required. In the presence of instrument noise, the weights allow for a heuristic pixel-noise weighting of the data. We start with the following estimators for the signal-plus-noise correlations:

$$\hat{C}_+(\psi) = A_P(\psi) \int d\hat{\mathbf{n}}_1 d\hat{\mathbf{n}}_2 [\delta(\hat{\mathbf{n}}_1 \cdot \hat{\mathbf{n}}_2 - \cos \psi) \times w_P(\hat{\mathbf{n}}_1) w_P(\hat{\mathbf{n}}_2) \bar{P}^*(\hat{\mathbf{n}}_1) \bar{P}(\hat{\mathbf{n}}_2)], \quad (28)$$

$$\hat{C}_-(\psi) = A_P(\psi) \int d\hat{\mathbf{n}}_1 d\hat{\mathbf{n}}_2 [\delta(\hat{\mathbf{n}}_1 \cdot \hat{\mathbf{n}}_2 - \cos \psi) \times w_P(\hat{\mathbf{n}}_1) w_P(\hat{\mathbf{n}}_2) \bar{P}(\hat{\mathbf{n}}_1) \bar{P}(\hat{\mathbf{n}}_2)], \quad (29)$$

$$\hat{C}_X(\psi) = A_X(\psi) \int d\hat{\mathbf{n}}_1 d\hat{\mathbf{n}}_2 [\delta(\hat{\mathbf{n}}_1 \cdot \hat{\mathbf{n}}_2 - \cos \psi) \times w_T(\hat{\mathbf{n}}_1) w_P(\hat{\mathbf{n}}_2) T(\hat{\mathbf{n}}_1) \bar{P}(\hat{\mathbf{n}}_2)]. \quad (30)$$

The delta functions ensure that we only consider those points that have angular separation  $\psi$ . The normalisations  $A(\psi)$  are chosen so that our correlation function estimators are unbiased in the absence of noise. This requires

$$\frac{1}{A_P(\psi)} = \int d\hat{\mathbf{n}}_1 d\hat{\mathbf{n}}_2 [\delta(\hat{\mathbf{n}}_1 \cdot \hat{\mathbf{n}}_2 - \cos \psi) \times w_P(\hat{\mathbf{n}}_1) w_P(\hat{\mathbf{n}}_2)], \quad (31)$$

$$\frac{1}{A_X(\psi)} = \int d\hat{\mathbf{n}}_1 d\hat{\mathbf{n}}_2 [\delta(\hat{\mathbf{n}}_1 \cdot \hat{\mathbf{n}}_2 - \cos \psi) \times w_T(\hat{\mathbf{n}}_1) w_P(\hat{\mathbf{n}}_2)]. \quad (32)$$

These expressions for the correlation functions and normalisation factor can be simplified by using the completeness relation

$$\sum_{l \geq \max(|m|, |n|)} \frac{2l+1}{2} d_{mn}^l(\beta) d_{mn}^l(\psi) = \delta(\cos \beta - \cos \psi) \quad (33)$$

to substitute for the delta functions. To evaluate  $\hat{C}_+(\psi)$  we set  $m = n = 2$ , so the integrand in equation (28) involves

$$w_P(\hat{\mathbf{n}}_1) \bar{P}^*(\hat{\mathbf{n}}_1) d_{22}^l(\beta) \bar{P}(\hat{\mathbf{n}}_2) w_P(\hat{\mathbf{n}}_2) = \tilde{P}^*(\hat{\mathbf{n}}_1) D_{22}^l(\alpha, \beta, -\gamma) \tilde{P}(\hat{\mathbf{n}}_2), \quad (34)$$

where  $\cos \beta = \hat{\mathbf{n}}_1 \cdot \hat{\mathbf{n}}_2$ , and we have used equations (11) and (12). Here,  $\tilde{P}(\hat{\mathbf{n}}) \equiv w_P(\hat{\mathbf{n}}) P(\hat{\mathbf{n}})$  is the weighted polarization field on the (polar-)coordinate basis. We can now use equation (7) to express the  $D$ -matrix in terms of spin-weight harmonics. Performing the angular integrals extracts the spin-weight 2 (pseudo-)multipoles of the weighted, noisy polarization field, defined by

$$\tilde{P}(\hat{\mathbf{n}}) = \sum_{lm} (\tilde{E}_{lm} - i\tilde{B}_{lm})_{-2} Y_{lm}(\hat{\mathbf{n}}), \quad (35)$$

$$\tilde{P}^*(\hat{\mathbf{n}}) = \sum_{lm} (\tilde{E}_{lm} + i\tilde{B}_{lm})_{+2} Y_{lm}(\hat{\mathbf{n}}), \quad (36)$$

leaving

$$\hat{C}_+(\psi) = 2\pi A_P(\psi) \sum_{lm} d_{22}^l(\psi) |\tilde{E}_{lm} + i\tilde{B}_{lm}|^2. \quad (37)$$

Introducing the real pseudo- $C_l$ s for the weighted fields:

$$\tilde{C}_l^E \equiv \frac{1}{2l+1} \sum_m |\tilde{E}_{lm}|^2, \quad (38)$$

$$\tilde{C}_l^B \equiv \frac{1}{2l+1} \sum_m |\tilde{B}_{lm}|^2, \quad (39)$$

$$\tilde{C}_l^{EB} \equiv \frac{1}{2l+1} \sum_m \tilde{E}_{lm} \tilde{B}_{lm}^* = \frac{1}{2l+1} \sum_m \tilde{B}_{lm} \tilde{E}_{lm}^*, \quad (40)$$

$$\tilde{C}_l^{TB} \equiv \frac{1}{2l+1} \sum_m \tilde{T}_{lm} \tilde{B}_{lm}^* = \frac{1}{2l+1} \sum_m \tilde{B}_{lm} \tilde{T}_{lm}^*, \quad (41)$$

we can write

$$\hat{C}_+(\psi) = 2\pi A_P(\psi) \sum_l (2l+1) d_{22}^l(\psi) (\tilde{C}_l^E + \tilde{C}_l^B). \quad (42)$$

To evaluate  $\hat{C}_-(\psi)$  we follow the same procedure, but with  $m = -2$  and  $n = 2$  in equation (33). The result is

$$\hat{C}_-(\psi) = 2\pi A_P(\psi) \sum_l (2l+1) d_{2-2}^l(\psi) (\tilde{C}_l^E - \tilde{C}_l^B - 2i\tilde{C}_l^{EB}). \quad (43)$$

Finally, for  $\hat{C}_X(\psi)$  we take  $m = 2$  and  $n = 0$  to find

$$\hat{C}_X(\psi) = 2\pi A_X(\psi) \sum_l (2l+1) d_{20}^l(\psi) (\tilde{C}_l^{TE} - i\tilde{C}_l^{TB}). \quad (44)$$

The normalisation factors  $A(\psi)$  can be evaluated by taking  $m = n = 0$  in equation (33), e.g.

$$\frac{1}{A_P(\psi)} = 2\pi \sum_{l \geq 0} (2l+1) P_l(\cos \psi) w_{P,l}, \quad (45)$$

where

$$w_{P,l} = \frac{1}{2l+1} \sum_m |w_{P,lm}|^2, \quad (46)$$

with  $w_{P,lm}$  the (spin-0) spherical multipoles of the weight function  $w_P(\hat{\mathbf{n}})$ . Note that we have used  $d_{00}^l(\psi) = P_l(\cos \psi)$  where  $P_l(x)$  is a Legendre polynomial. Once the mean noise contribution (noise bias) is removed from the estimators  $\hat{C}(\psi)$  [leaving unbiased estimators of the signal correlation functions  $\xi(\psi)$ ], we can use equations (25)–(27) to compute estimates of the power spectra. The real parts of  $\hat{\xi}(\psi)$  give estimates of  $C_l^E$ ,  $C_l^B$  and  $C_l^X$ , while the imaginary parts of  $\hat{\xi}_-(\psi)$  and  $\hat{\xi}_X(\psi)$  can be used to estimate  $C_l^{EB}$  and  $C_l^{TB}$  and hence test for parity violations.

The full set of pseudo-multipoles can be obtained efficiently in  $O(N_{\text{pix}}^{3/2} \log N_{\text{pix}})$  operations using fast spherical transforms such as those implemented in the HEALPix<sup>5</sup> and IGLOO(Crittenden & Turok 1998) packages. (Our current implementation employs HEALPix.) To remove the noise bias from  $\hat{C}(\psi)$  it is generally most efficient to resort to Monte-Carlo simulations of pure noise fields (Szapudi et al. 2001). (An exception is the case where the noise is uncorrelated between pixels; see below for details.) The ensemble mean of these pure-noise correlation functions can be subtracted from  $\hat{C}(\psi)$  to yield (asymptotically) unbiased estimates of the signal correlation functions. Monte-Carlo estimation of the noise bias provides a robust means of dealing with discretisation effects due to the chosen pixelisation. Monte-Carlo methods also offer the simplest method of computing the variance of the power spectrum estimates. In the presence of uncorrelated noise it is straightforward to proceed analytically with the noise contribution to the variance, but the cosmic variance contribution is complicated by the presence of signal correlations.

For the simple case of noise that is uncorrelated between

pixels it is straightforward to compute the noise bias analytically. For simplicity consider noise that is uncorrelated between  $Q$ ,  $U$  and  $T$ , and has equal variance in  $Q$  and  $U$ . If the noise variance of the Stokes parameters per solid angle is  $\sigma_P^2(\hat{\mathbf{n}}_p)$ , then in the continuum limit the polarization noise correlations can be summarised by

$$\langle P_N(\hat{\mathbf{n}}_1) P_N^*(\hat{\mathbf{n}}_2) \rangle = 2\sigma_P^2 \delta(\hat{\mathbf{n}}_1 - \hat{\mathbf{n}}_2), \quad (47)$$

$$\langle P_N(\hat{\mathbf{n}}_1) P_N(\hat{\mathbf{n}}_2) \rangle = 0, \quad (48)$$

$$\langle T_N(\hat{\mathbf{n}}_1) P_N(\hat{\mathbf{n}}_2) \rangle = 0, \quad (49)$$

where  $P_N(\hat{\mathbf{n}})$  is the spin  $-2$  noise, and  $T_N(\hat{\mathbf{n}})$  is the noise on the temperature. As the noise is uncorrelated between pixels its mean effect on correlation function estimates is confined to zero separation:

$$\begin{aligned} \langle \Delta \hat{C}_+(\psi) \rangle &= A_P(0) \delta(1 - \cos \psi) \\ &\quad \times \int d\hat{\mathbf{n}} w_P^2(\hat{\mathbf{n}}) 2\sigma_P^2(\hat{\mathbf{n}}), \end{aligned} \quad (50)$$

$$\langle \Delta \hat{C}_-(\psi) \rangle = 0, \quad (51)$$

$$\langle \Delta \hat{C}_X(\psi) \rangle = 0, \quad (52)$$

with

$$\frac{1}{A_P(0)} = 2\pi \int d\hat{\mathbf{n}} w_P^2(\hat{\mathbf{n}}). \quad (53)$$

Here,  $\langle \Delta \hat{C} \rangle$  is the mean noise contribution to the estimators  $\hat{C}$ . Making use of  $d_{mm'}^l(0) = \delta_{mm'}$  we find that the non-zero noise biases in the estimates of the power spectra in the continuum limit are

$$\langle \Delta \hat{C}_l^E \rangle = \langle \Delta \hat{C}_l^B \rangle = \frac{\int d\hat{\mathbf{n}} w_P^2(\hat{\mathbf{n}}) \sigma_P^2(\hat{\mathbf{n}})}{\int d\hat{\mathbf{n}} w_P^2(\hat{\mathbf{n}})}. \quad (54)$$

However, we would recommend removing the noise bias with Monte-Carlo techniques even for simple, uncorrelated noise. This is to ensure that the effective band limit introduced on the noise by computing the correlation functions via pseudo- $C_l$ s up to some finite  $l_{\text{max}}$  is properly accounted for.

### 3.1 Application to large-area surveys

As an application of our method we consider extracting the power spectra from simulated maps obtained with a full-sky survey with pixel noise similar to that expected for *Planck*. To be specific, we assumed uncorrelated pixel noise on  $Q$  and  $U$  with r.m.s.  $6.95 \mu\text{K}$  in a 10-arcmin by 10-arcmin pixel. We adopted a beam size of 10 arcmin, somewhat larger than the polarization-sensitive channels of the *Planck* High-Frequency Instrument, so to ensure oversampling of the beam at HEALPix resolution  $N_{\text{side}} = 1024$ . We ignored the variation in pixel noise across the map, but this could easily be included in our simulations at no additional computational cost. Noise correlations could also be included easily if fast simulation of noise realisations were possible. We made a constant-latitude Galactic cut of  $\pm 20^\circ$ . The underlying cosmological model was as described in Sec. 1 and we assumed reionization at  $z = 6$ . We adopted a uniform weighting scheme motivated by the constant variance of the noise.

The recovered power spectrum  $C_l^E$  is shown in Fig. 2. We computed estimates of the correlation function at the

<sup>5</sup> <http://www.eso.org/science/healpix/>

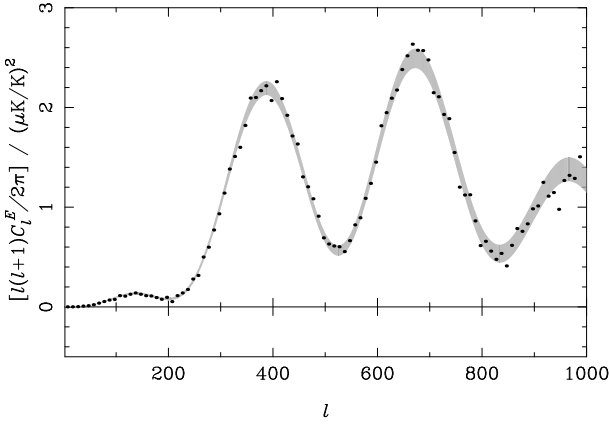


**Figure 2.** Recovered  $C_l^E$  power spectrum for a large-area survey with a  $\pm 20^\circ$  Galactic cut. The points are flat band-power estimates, with  $\Delta l = 10$ , from a single simulation; the shaded region shows the  $\pm\sigma$  region on the basis of equation (55).

roots of a Legendre polynomial from the pseudo- $C_l$ s (obtained with the fast spherical transforms in HEALPix). Inversion of the correlation functions was performed with Gauss-Legendre integration. We averaged the recovered  $l(l+1)C_l$  to form flat band-power estimates with a  $\Delta l = 10$ , and the results of one simulation are shown as the points in Fig. 2. We adopted a  $\Delta l = 10$  to ensure the errors were essentially uncorrelated. The shaded area in Fig. 2, centred on the true spectrum smoothed with a 10-arcmin beam, encloses the  $\pm\sigma$  error region based on the rule of thumb (generalised from Hivon et al. 2002 for the temperature case)

$$\Delta C_l^E \approx \sqrt{\frac{2}{\nu_l}} (C_l^E + N_l). \quad (55)$$

Here  $N_l$  is the (full-sky) noise power spectrum, and  $\nu_l \equiv \Delta l(2l+1)f_{\text{sky}}w_2^2/w_4$  is the effective number of degrees of freedom in a band of width  $\Delta l$  on a fraction of the sky  $f_{\text{sky}}$ , where  $4\pi w_i f_{\text{sky}} \equiv \int w_P^i(\hat{n}) d\hat{n}$ . Note that  $\nu_l$  takes no account of the loss of degrees of freedom associated with disentangling  $E$  and  $B$  polarization, since the fractional loss of modes is small for  $f_{\text{sky}}$  close to unity (Lewis et al. 2002). The scatter of points in the simulation is broadly consistent with that expected on the basis of the theoretical errors. A more detailed analysis of the optimality of our method must await comparison with optimal, maximum-likelihood codes when these become available at sufficiently high resolution.

#### 4 WINDOW FUNCTIONS FROM INCOMPLETE CORRELATION FUNCTIONS

In this section we construct the window functions that arise when the correlation functions can only be estimated over a limited angular range. We shall concentrate on the polarization auto-correlations; the generalisation to the polarization-temperature cross-correlation is straightforward.

If unbiased estimates of the correlation functions are available over the full angular range  $(0, \pi)$ , they can easily be inverted to obtain unbiased power spectra. This case would describe full-sky experiments with a cut excising less than a  $90^\circ$  band about the Galactic plane. In the case where the correlation functions cannot be estimated for all separations

$\psi$ , estimating the power spectra by direct integration (e.g. equations 25 and 26) over the observed range will introduce window functions  ${}_{\pm 2}K_{ll'}$  such that

$$\langle \hat{C}_l^E \pm \hat{C}_l^B \rangle = \sum_{l'} {}_{\pm 2}K_{ll'} (C_{l'}^E \pm C_{l'}^B). \quad (56)$$

Fourier ringing can be reduced by pre-multiplying the correlation functions with a scalar apodizing function  $f(\psi)$  prior to integration, in which case the window functions take the form

$${}_{\pm 2}K_{ll'} \equiv \frac{2l'+1}{2} \int f(\beta) d_{\pm 2}^l(\beta) d_{\pm 2}^{l'}(\beta) d\cos\beta, \quad (57)$$

where the integral is over the range of angles for which the correlation functions can be estimated. Note that the window functions are not symmetric but rather satisfy

$$(2l+1) {}_{\pm 2}K_{ll'} = (2l'+1) {}_{\pm 2}K_{l'l}. \quad (58)$$

Introducing the sum and difference window functions,  ${}_{\pm}K_{ll'} \equiv ({}_{2}K_{ll'} \pm {}_{-2}K_{ll'})/2$ , the means of the estimated power spectra are related to the true spectra by

$$\langle \hat{C}_l^E \rangle = \sum_{l'} ({}_{+}K_{ll'} C_{l'}^E + {}_{-}K_{ll'} C_{l'}^B), \quad (59)$$

$$\langle \hat{C}_l^B \rangle = \sum_{l'} ({}_{-}K_{ll'} C_{l'}^E + {}_{+}K_{ll'} C_{l'}^B). \quad (60)$$

The window function  ${}_{-}K_{ll'}$  controls the mixing of  $E$  and  $B$  polarization. Recent results from DASI (Kovac et al. 2002) are in line with theoretical expectations that  $B$  polarization should be sub-dominant, so that cross contamination due to partial sky effects is proportionately more troubling for  $B$  polarization than for  $E$ . While not presenting a fundamental problem for cosmological parameter extraction, a non-zero  ${}_{-}K_{ll'}$  makes interpretation (and presentation) of the estimated  $C_l^B$  awkward. Mixing can obviously be eliminated by pre-multiplying the estimates  $\hat{C}_l^E \pm \hat{C}_l^B$  with the inverse of the window functions  ${}_{\pm 2}K_{ll'}$ , but this inversion is awkward in practice due to the ill-conditioned nature of the window functions when coverage of the correlation functions is incomplete. In Section 5 we introduce a simple, robust technique for extracting the power spectra from correlation functions which eliminates mixing in the mean (i.e. produces a zero  ${}_{-}K_{ll'}$ ). Before turning to that, in the following subsections we first explore the properties of the window functions given by equation (57), and the circumstances under which mixing is significant.

##### 4.1 General properties

If we define the apodizing function  $f(\psi)$  to be zero outside the observed range of  $\psi$ , and perform a Legendre expansion

$$f(\psi) = \sum_{l \geq 0} \frac{2l+1}{2} f_l P_l(\cos\psi), \quad (61)$$

the window function  ${}_{2}K_{ll'}$  reduces to

$${}_{2}K_{ll'} = \frac{2l'+1}{2} \sum_L (2L+1) f_L \begin{pmatrix} l & l' & L \\ 2 & -2 & 0 \end{pmatrix}^2, \quad (62)$$

while  ${}_{-2}K_{ll'}$  has an additional factor of  $(-1)^{(l+l'+L)}$  in the summation. The array in brackets in equation (62) is a

Wigner 3- $j$  symbol arising from the integral of a product of three rotation matrices. If the apodizing function is effectively band limited to  $L_{\max}$ , the window functions vanish for  $|l - l'| > L_{\max}$ .

The normalisation  $\sum_{l'} {}_2K_{ll'}$  of the window functions is also of some interest. For  ${}_2K_{ll'}$  we can perform the sum over  $l'$  in equation (62) directly using the orthogonality of the 3- $j$  symbols (Varshalovich et al. 1988) to find

$$\sum_{l'} {}_2K_{ll'} = \sum_{L \geq 0} \frac{2L+1}{2} f_L = f(0). \quad (63)$$

The last equality follows from  $P_1(1) = 1$ , or, more directly, by employing  $\sum_{l'} (l' + 1/2) d_{22}^{l'}(\beta) = \delta(\cos \beta - 1)$  in equation (57). The normalisation of  ${}_2K_{ll'}$  is a little more involved. We start with the result

$$\sum_{l'} \frac{2l'+1}{2} d_{2-2}^{l'}(\beta) = \delta(\cos \beta - 1) + \csc^2(\beta/2), \quad (64)$$

which follows by summing equation (89) of Section 5 over  $l'$ . If we now sum equation (57) over  $l'$ , and use equation (64), we find that

$$\sum_{l'} {}_2K_{ll'} = \int f(\beta) \csc^2(\beta/2) d_{2-2}^l(\beta) d \cos \beta, \quad (65)$$

where we have used  $d_{2-2}^l(0) = 0$  [and the assumed regularity of  $f(\beta)$ ]. The function  $\csc^2(\beta/2) d_{2-2}^l(\beta)$  is a polynomial in  $\cos \beta$  and so the integral can easily be evaluated numerically by e.g. Gauss-Legendre integration for smooth apodizing functions. To make further progress analytically we insert the Legendre expansion of  $f(\beta)$  in equation (65) and use the differential representation of the reduced  $D$ -matrices (e.g. Section 4.3.2 of Varshalovich et al. 1988). Repeated integration by parts then establishes the result

$$\begin{aligned} \sum_{l'} {}_2K_{ll'} &= \sum_{L \leq l} \frac{2L+1}{2} f_L \left( 1 - 4 \frac{L(L+1)}{l(l+1)} \right. \\ &\quad \left. + 3 \frac{(L+2)!(l-2)!}{(L-2)!(l+2)!} \right). \end{aligned} \quad (66)$$

If  $f(\beta)$  is effectively band-limited, for  $l \gg L_{\max}$  we have  $\sum_{l'} {}_2K_{ll'} \approx f(0)$ . In this limit, the normalisation of  ${}_2K_{ll'}$  is much smaller than that of  ${}_+K_{ll'}$ , and mixing of  $E$  and  $B$ -power is suppressed in the mean (Bunn 2002).

## 4.2 No apodization

Consider the case where the correlation functions can be estimated in the range  $(0, \beta_{\max})$ . If we apply no apodization to the correlation functions, we obtain window functions

$${}_2W_{ll'} \equiv \frac{2l'+1}{2} \int_{\cos \beta_{\max}}^1 d_{2\pm 2}^{l'}(\beta) d_{2\pm 2}^l(\beta) d \cos \beta. \quad (67)$$

For  $l \neq l'$  this integral can be evaluated directly since the  $d_{mn}^l$  are eigenfunctions of a self-adjoint operator. The result is

$$\begin{aligned} {}_2W_{ll'} &= \frac{2l'+1}{2} \frac{\cos^2 \beta_{\max}}{l(l+1) - l'(l'+1)} \left( \frac{d d_{2\pm 2}^{l'}(\beta)}{d \cos \beta} d_{2\pm 2}^l(\beta) \right. \\ &\quad \left. - \frac{d d_{2\pm 2}^l(\beta)}{d \cos \beta} d_{2\pm 2}^{l'}(\beta) \right) \Big|_{\beta_{\max}}, \quad l \neq l'. \end{aligned} \quad (68)$$

For  $l = l'$  the integral can be evaluated recursively as described in Appendix C of Lewis et al. (2002). The window function  ${}_2W_{ll'} \equiv ({}_+W_{ll'} - {}_-W_{ll'})/2$  can be evaluated directly for all  $l$  and  $l'$  (Lewis et al. 2002):

$${}_2W_{ll'} = \frac{2l'+1}{2} (u_l u_{l'} + v_l v_{l'})|_{\beta_{\max}}, \quad (69)$$

where the vectors

$$u_l(\beta) \equiv \sqrt{\frac{(l-2)!}{(l+2)!}} \sin \beta \frac{d}{d\beta} \left( \frac{d_{20}^l}{\sin \beta} \right), \quad (70)$$

$$v_l(\beta) \equiv \sqrt{\frac{(l-2)!}{(l+2)!}} \frac{\sqrt{3}}{\sin \beta} d_{20}^l(\beta). \quad (71)$$

Both vectors vanish for  $\beta_{\max} = \pi$  to ensure that  ${}_2W_{ll'} = 0$  when the full angular range  $(0, \pi)$  is considered.

Some representative rows of the window functions  $\pm W_{ll'}$  are shown in Fig. 3 for  $\beta_{\max} = 20^\circ$  (corresponding to e.g. observations over a circular patch of radius  $10^\circ$ ). Note that  ${}_+W_{ll'}$  is localised around  $l = l'$  (with width varying inversely with  $\beta_{\max}$ ), while  ${}_2W_{ll'}$  shows no localisation. Equation (69) shows that, considered as a matrix,  ${}_2W_{ll'}$  is of rank 2, so the rows of the window function are constructed from linear combinations of  $u_{l'}$  and  $v_{l'}$ . The approximate scaling of  ${}_2W_{ll'}$  with  $l$  for fixed  $l'$ , that is evident in Fig. 3, arises because the vector  $u_l$  oscillates with larger amplitude than  $v_l$  for  $l \gtrsim 1/\beta_{\max}$ .

In Fig. 3 we also show the mean of the estimated power spectrum  $\langle \hat{C}_l^B \rangle$  obtained by multiplying the window functions  $\pm W_{ll'}$  with the true  $C_l^E$  and  $C_l^B$  (equation 60) for the cosmological models detailed in Sec. 1. The true spectra are convolved with a Gaussian beam of full-width 10 arcmin at half-maximum. In the case of no reionization, the mean of the recovered  $C_l^B$  is a faithful representation of the true spectra. This is because (i) the inner products between  $C_{l'}^E$  and either of  $(l' + 1/2)u_{l'}$  and  $(l' + 1/2)v_{l'}$  are sufficiently small that the leakage from  $E$  polarization causes only a small amplitude oscillation in the recovered  $C_l^B$ ; and (ii) for  ${}_+W_{ll'}$  sufficiently localised compared to the scale of features in  $C_{l'}^B$ , we can approximate their product by

$$\sum_{l'} {}_+W_{ll'} C_{l'}^B \approx C_l^B \sum_{l'} {}_+W_{ll'} \approx C_l^B \quad (l \gg 1/\beta_{\max}). \quad (72)$$

For the second approximation note that the window function  ${}_+W_{ll'}$  inherits its normalisation from that of  ${}_2W_{ll'}$  (which is unity) and  ${}_2W_{ll'}$ . For the latter we use equation (65) and the differential representation of  $d_{2-2}^l$  to find

$$\begin{aligned} \sum_{l'} {}_2W_{ll'} &= 1 + 2 \sqrt{\frac{(l-2)!}{(l+2)!}} \cot(\beta_{\max}/2) \\ &\quad \times \left[ \sqrt{l(l+1)} d_{1-2}^l(\beta) - \cot(\beta/2) d_{0-2}^l(\beta) \right]_{\beta_{\max}}. \end{aligned} \quad (73)$$

For large  $l \gg 1/\beta_{\max}$  we find  $\sum_{l'} {}_2W_{ll'} \approx 1$  (see also the discussion after equation 66). Reionized models are more problematic since they have additional large-scale power in  $E$  polarization (and so are more sensitive to the truncation of the correlation functions at  $\beta_{\max}$ ). The effect of this large-scale power can clearly be seen in Fig. 3 for the model with reionization at  $z = 6$ . The large amplitude oscillations in the recovered  $C_l^B$  trace those of the vector  $u_l(\beta_{\max})$  at large  $l$ .

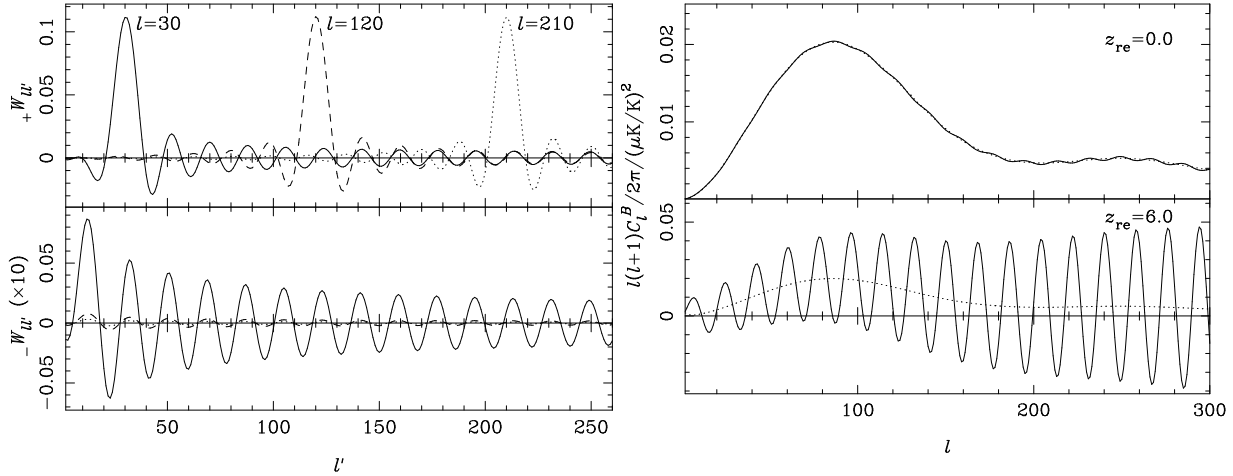


**Figure 3.** Left: representative rows of the window functions  $+W_{ll'}$  (top panel) and  $-W_{ll'}$  (bottom panel) when the correlation functions are known in the angular range  $(0, 20^\circ)$ , and no apodization is applied. The solid lines are for  $l = 30$ , the dashed for  $l = 120$  and the dotted for  $l = 210$ . Right: mean recovered  $C_l^B$  (solid lines), obtained from the convolution in equation (60) with the windows  $\pm W_{ll'}$ , compared to the true  $C_l^B$  (dashed lines). The top panel has no reionization while the bottom panel is a model with full reionization at  $z = 6$ .

### 4.3 Gaussian apodization

The Fourier ringing evident in the window functions in Fig. 3 can be reduced by apodizing the correlation functions. Here we consider Gaussian apodizing functions, i.e.

$$f(\beta) = e^{-\beta^2/(2\sigma^2)}. \quad (74)$$

The half-width at half-maximum is  $\sigma\sqrt{2\ln 2}$  which should be small compared to the cut off  $\beta_{\max}$  in the correlation functions for effective apodizing. The window functions, accounting for apodization and the finite range  $(0, \beta_{\max})$  of the observed correlation functions, can be written as matrix products:

$$\pm_2 K_{ll'} = \sum_L \pm_2 F_{lL} \pm_2 W_{Ll'}, \quad (75)$$

where

$$\pm_2 F_{ll'} \equiv \frac{2l' + 1}{2} \int_{-1}^1 f(\beta) d_{2\pm 2}^l(\beta) d_{2\pm 2}^{l'}(\beta) d\cos\beta. \quad (76)$$

Note that the full window functions  $\pm_2 K_{ll'}$  are insensitive to the behaviour of the apodizing function for  $\beta > \beta_{\max}$ . Note also that the order of the matrix product in equation (75) is irrelevant since the window functions commute. If the apodizing function is narrow compared to  $\beta_{\max}$  we expect  $\pm_2 K_{ll'} \approx \pm_2 F_{ll'}$ .

In Fig. 4 we show representative rows of the sum and difference window functions,  $\pm K_{ll'}$ , for  $\beta_{\max} = 20^\circ$  and a Gaussian apodizing function with half-width at half-maximum equal to  $\beta_{\max}/2$  [so  $f(\beta_{\max}) = 1/16$ ]. These are well approximated by Gaussians centred on  $l = l'$  with width  $1/\sigma$ . The amplitude of the difference window functions are much smaller than those of the sum, and for large  $l$  the ratio of amplitudes  $\propto 1/(l\sigma)^2$ .

To understand this behaviour, consider the limit where  $\sigma \ll 1$  and  $l\sigma \gg 1$ . In this flat-sky limit we can approximate the reduced  $D$ -matrices by Bessel functions (Varshalovich et al. 1988):

$$d_{22}^l(\beta) \approx J_0(l\beta), \quad d_{2-2}^l(\beta) \approx J_4(l\beta), \quad (77)$$

and the window functions  $\pm_2 F_{ll'}$  are easily computed to be

$${}_2F_{ll'} \approx l'\sigma^2 e^{-\sigma^2(l^2+l'^2)/2} I_0(ll'\sigma^2), \quad (78)$$

$$-{}_2F_{ll'} \approx l'\sigma^2 e^{-\sigma^2(l^2+l'^2)/2} I_4(ll'\sigma^2). \quad (79)$$

The leading-order asymptotic expansions of  $\pm F_{ll'}$  ( $ll'\sigma^2 \gg 1$ ) then follow:

$$+F_{ll'} \sim \sqrt{\frac{l'\sigma^2}{2\pi l}} e^{-(l-l')^2\sigma^2/2}, \quad (80)$$

$$-F_{ll'} \sim \frac{4}{ll'\sigma^2} \sqrt{\frac{l'\sigma^2}{2\pi l}} e^{-(l-l')^2\sigma^2/2}, \quad (81)$$

which reproduce the behaviour seen in Fig. 4. The window function  ${}_2F_{ll'}$  is normalised to unity by virtue of equation (63). The normalisation of  $-{}_2F_{ll'}$  can be calculated for all  $l$  in terms of modified spherical Bessel functions by approximating  $f(\beta) \approx \exp[-(1 - \cos\beta)/\sigma^2]$  in equation (65). However, the result is cumbersome so we shall only give its asymptotic form here (valid for  $\sigma \ll 1$  and  $l\sigma \gg 1$ ):

$$\sum_{l'} -{}_2F_{ll'} = 1 - \frac{4}{l^2\sigma^2} \left( 2 + e^{-l^2\sigma^2/2} \right) + \frac{24}{l^4\sigma^4} \left( 1 - e^{-l^2\sigma^2/2} \right). \quad (82)$$

(This result also follows directly from integrating equation 79 over  $l'$ .) Asymptotically, we then have  $\sum_{l'} -F_{ll'} \sim 4/(l\sigma)^2$ , consistent with Fig. 3.

We also show in Fig. 4 the mean of the recovered  $C_l^B$  for a range of  $l$  values with Gaussian apodizing (corresponding to the window functions in the left-hand panels of Fig. 4). The spacing of points is chosen to reflect the  $l$ -range over which recovered power spectra should be roughly decorrelated. While apodizing has clearly removed the high-frequency oscillations in the mean of the recovered  $C_l^B$ , it has done so at the expense of introducing considerable bias due to leakage from  $E$  polarization. As expected, apodization has reduced the sensitivity of the recovered  $C_l^B$  to the level of large-scale power in  $E$  polarization (and hence reion-

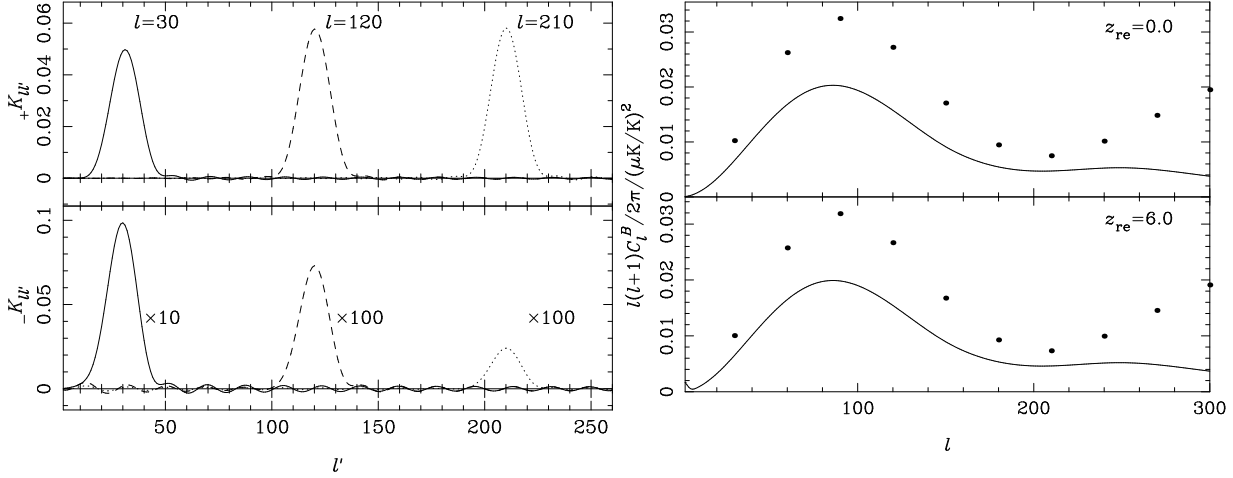


**Figure 4.** Left: representative rows of  $\pm K_{lW}$  for  $\beta_{\max} = 20^\circ$  and Gaussian apodization with half-width at half-maximum equal to  $\beta_{\max}/2$ . Right: mean recovered  $C_l^B$  (points) compared to the true  $C_l^B$  (lines) with (bottom) and without (top) reionization.

ization; c.f. Fig. 3), but has replaced it with a local bias  $\approx 4C_l^E/(l\sigma)^2$ . The bias becomes non-local in models with sufficiently early reionization, where the level of large-scale  $E$  power can be such that it is transmitted to the recovered  $B$  power spectrum for all  $l$  through the low- $l$  tail of the window function.

A more effective way to reduce oscillations in  $C_l^B$  without introducing additional bias due to  $E$ - $B$  leakage is to recover the power spectra with no apodization, and then to post-convolve with a suitably-wide smoothing function. Such an approach is illustrated in Fig. 5, where we have post-convolved the results in Fig. 3 with the asymptotic form of  $+F_{lW}$  (equation 80). The Gaussian smoothing produces well-localised  $+K_{lW}$  window functions, removing the Fourier ringing from  $+W_{lW}$ , and reduces the amplitude of  $-W_{lW}$  by a factor  $\sim 40$ . Only a low-frequency, oscillatory bias remains in the recovered  $C_l^B$  in the model with reionization. Whether this bias is significant depends on the level of reionization (and primordial  $B$  polarization).

## 5 REMOVING $E$ - $B$ LEAKAGE

Although we are able to reduce the level of cross-contamination in the recovered power spectra by simply post-convolving them with a suitably-wide smoothing function, it is actually straightforward to remove this  $E$ - $B$  mixing exactly in the mean. Crittenden et al. (2002) showed how to construct correlation functions on small patches of the sky that contain only  $E$  or only  $B$  modes in the mean. (Their work was in the context of weak gravitational lensing, but their results are equally applicable to CMB polarization.) In this section we extend the central result of Crittenden et al. to the sphere, so we are able to handle large-angle polarization signals, and demonstrate the methods with simulations for an experiment similar to BICEP.

We begin by considering the function

$$\xi(\beta) \equiv \sum_l \frac{2l+1}{4\pi} (C_l^E + C_l^B) d_{2-2}^l(\beta). \quad (83)$$

If we had access to  $\xi(\beta)$  over some range of scales we could combine with the real part of  $\xi_-(\beta)$  to extract the function

$$\frac{1}{2}[\xi(\beta) - \Re\xi_-(\beta)] = \sum_l \frac{2l+1}{4\pi} C_l^B d_{2-2}^l(\beta), \quad (84)$$

which depends only on  $B$ -polarization. We could thus recover an estimate of  $C_l^B$  by integrating unbiased estimates of  $\xi(\beta) - \xi_-(\beta)$  against  $d_{2-2}^l$  [with appropriate apodization  $f(\beta)$ ]:

$$\hat{C}_l^B = 2\pi \int \frac{1}{2} [\hat{\xi}(\beta) - \Re\hat{\xi}_-(\beta)] f(\beta) d_{2-2}^l(\beta) d\cos\beta. \quad (85)$$

Such an estimate would contain no contamination from  $E$  polarization in the mean (i.e. the difference window function  $-K_{lW}$  would vanish for arbitrary apodization). A similarly unbiased estimate of  $C_l^E$  could be obtained by considering  $\xi(\beta) + \Re\xi_-(\beta)$ .

The result we now prove is that the function  $\xi(\beta)$  can be obtained in the range  $(0, \beta_{\max})$  from the correlation function  $\xi_+(\beta)$  in the same range by quadrature. We start by inserting equation (26) into the summand of equation (83) which gives

$$\xi(\beta) = \int_{-1}^1 d\cos\beta' \xi_+(\beta') \sum_l \frac{2l+1}{2} d_{2-2}^l(\beta) d_{22}^l(\beta'). \quad (86)$$

Our strategy for simplifying the summation in this equation is to express  $d_{2-2}^l(\beta)$  in terms of integrals involving  $d_{22}^l(\beta)$ , and then perform the summation with the completeness relation, equation (33). Making repeated use of the recursion relation (Varshalovich et al. 1988)

$$\begin{aligned} \frac{-m+m'\cos\beta}{\sin\beta} d_{mm'}^l(\beta) &= \frac{1}{2} \sqrt{(l+m')(l-m'+1)} d_{mm'-1}^l(\beta) \\ &+ \frac{1}{2} \sqrt{(l-m')(l+m'+1)} d_{mm'+1}^l(\beta) \end{aligned} \quad (87)$$

and the relation

$$\begin{aligned} \frac{d}{d\beta} d_{mm'}^l(\beta) + \frac{m-m'\cos\beta}{\sin\beta} d_{mm'}^l(\beta) \\ = -\sqrt{(l-m')(l+m'+1)} d_{mm'+1}^l(\beta), \end{aligned} \quad (88)$$

we find that

$$d_{2-2}^l(\beta) = d_{22}^l(\beta) - \frac{2(2+\cos\beta)}{\sin^4(\beta/2)} \int_0^\beta \tan^3(\beta'/2) d_{22}^l(\beta') d\beta'$$

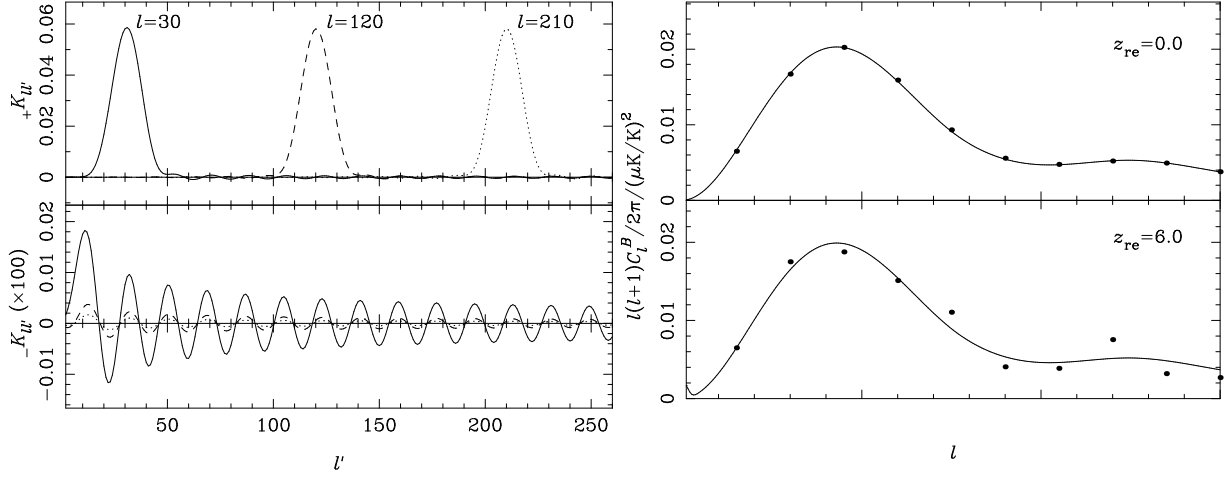


**Figure 5.** Window functions (left) and mean of recovered  $C_l^B$  (right) obtained by post-convolving the results in Fig. 3 with the Gaussian asymptotic approximation to  ${}_+F_{ll}$ .

$$+ \frac{2}{\sin^2(\beta/2)} \int_0^\beta \sec^3(\beta'/2) \sin(\beta'/2) d_{22}^l(\beta') d\beta'. \quad (89)$$

Multiplying with  $(l+1/2)d_{22}^l(\beta')$  and summing over  $l$  we find

$$\begin{aligned} \xi(\beta) &= \xi_+(\beta) + \frac{1}{\sin^2(\beta/2)} \int_{\cos \beta}^1 d \cos \beta' \xi_+(\beta') \sec^4(\beta'/2) \\ &- \frac{2(2 + \cos \beta)}{\sin^4(\beta/2)} \int_{\cos \beta}^1 d \cos \beta' \xi_+(\beta') \frac{\tan^3(\beta'/2)}{\sin \beta'}. \end{aligned} \quad (90)$$

As  $\xi(\beta)$  depends only on  $\xi_+(\beta)$  in the range  $(0, \beta)$ , it is possible to construct  $\xi(\beta)$  in this range from an unbiased estimator of  $\xi_+(\beta)$  in the same range. By construction,  $\xi(\beta) - \Re \xi_-(\beta)$  will contain only  $B$  polarization in the mean.

The window function for this method is simply  ${}_2K_{ll}$  (equation 57), so that

$$\langle \hat{C}_l^B \rangle = \sum_{l'} {}_2K_{ll'} C_{l'}^B, \quad \langle \hat{C}_l^E \rangle = \sum_{l'} {}_2K_{ll'} C_{l'}^E. \quad (91)$$

As in the previous section, we can write  ${}_2K_{ll} = \sum_L {}_2F_{lL} {}_2W_{Ll}$ . Representative elements of the window functions  ${}_2K_{ll'}$  are plotted in Fig. 6 for  $\beta_{\max} = 20^\circ$  and Gaussian apodizing with half-width at half-maximum equal to  $\beta_{\max}/2$ . They are well approximated by Gaussians with asymptotic normalisation given by the right-hand side of equation (82). For presentation purposes it is desirable to have window functions normalised to unity. We can enforce this by dividing the power spectrum reconstructed from equation (85) by  $\sum_{l'} {}_2K_{ll'}$ . The exact normalisation is easily computed from equation (65) by e.g. Gauss-Legendre integration, and can be performed while inverting the correlation functions at negligible computational cost. The renormalised window functions are also shown in Fig. 6, along with the mean recovered  $C_l^B$ , obtained from equation (85) with and without renormalisation by  $\sum_{l'} {}_2K_{ll'}$ . The renormalised estimates agree very well in the mean with the true power spectra. Note also that since we have removed cross-contamination, the recovered  $C_l^B$  are insensitive to large-scale power (from reionization) in  $E$  polarization.

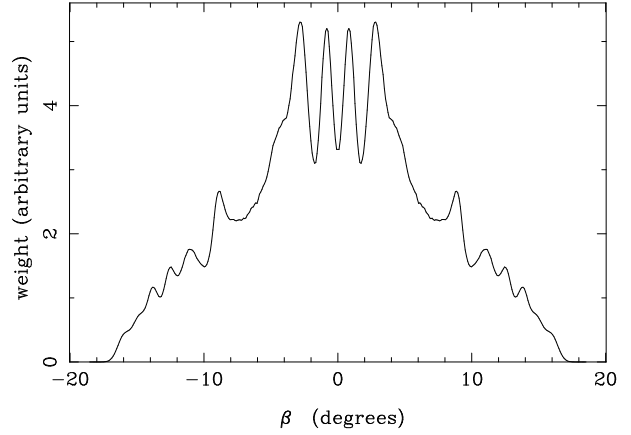


**Figure 7.** Azimuthally-symmetric weight function  $w_P(\hat{n})$  adopted for the BICEP simulations. We chose to weight in proportion to the integration time per pixel. For white noise this is equivalent to weighting with the inverse of the noise variance.

### 5.1 Application to BICEP

As an application of our new estimator, we consider simulated maps for the BICEP experiment. BICEP is the first of a new generation of large bolometer arrays that are designed to target  $B$ -mode polarization. We used the experimental parameters taken from the BICEP homepage<sup>6</sup>. The survey will cover a polar-cap region of angular radius  $18^\circ 5'$ , integrating for a nominal 300 days. BICEP will be composed of 48 polarization-sensitive bolometers (PSBs) operating at 100 GHz with a resolution of  $1^\circ$  (full-width at half-maximum) and 48 at 150 GHz with  $0^\circ 7'$  resolution. For our simulations we ignored the difference in beam size between the two channels taking the beam size to be  $1^\circ$ , so maps from each channel could be easily combined without introducing noise correlations. We took each PSB to have an instantaneous sensitivity of  $300 \mu\text{K}\sqrt{\text{sec}}$ .

We simulated 100 noisy CMB maps using a realistic map of the integration time per pixel based on the BICEP

<sup>6</sup> <http://bicep.caltech.edu>

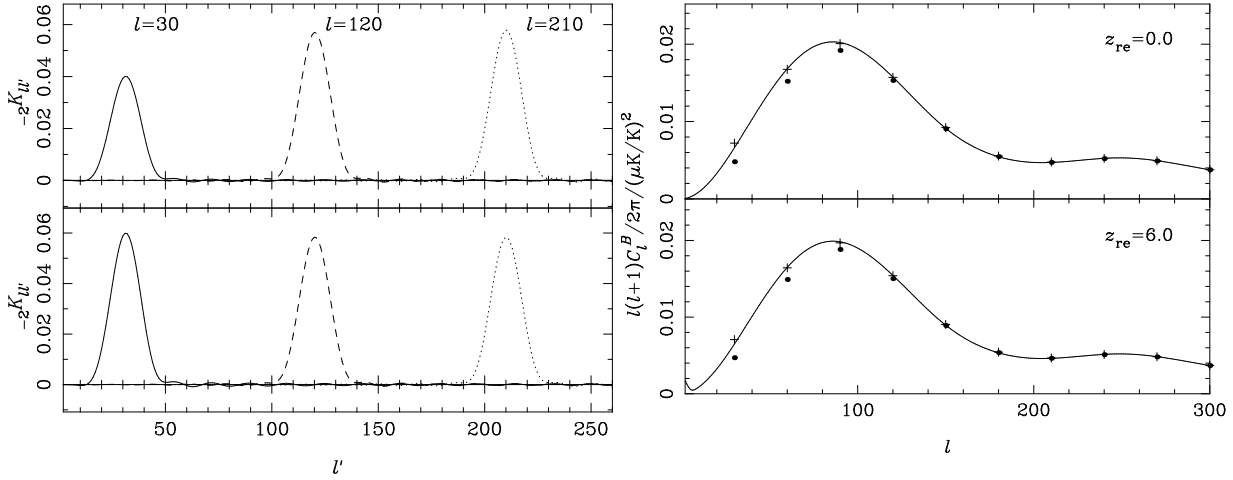


**Figure 6.** Left: window functions  $-2K_{ll'}$  (top) and their renormalised counterparts (bottom) for  $\beta_{\max} = 20^\circ$  and Gaussian apodization with half-width at half-maximum equal to  $\beta_{\max}/2$ . Right: mean recovered  $C_l^B$  with (crosses) and without (circles) renormalisation for the cosmological models with (bottom) and without (top) reionization.

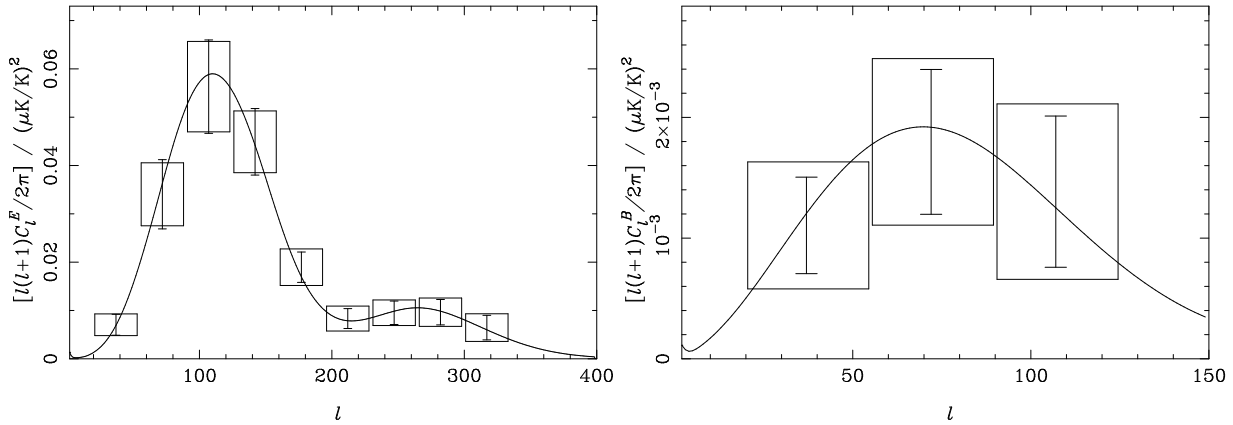


**Figure 8.** The mean in 100 BICEP simulations of the flat band-powers for  $C_l^E$  (left; smoothed with a 1-degree beam) and  $C_l^B$  (right). Monte-Carlo error estimates from the 100 simulations are shown as boxes, centred on the average bandpowers from the simulations. The error bars are the theoretical approximation in equation (92). The solid lines are the input theoretical spectra, smoothed with the beam, for the cosmological model described in Sec. 1 with reionization at  $z = 6$ . Note they are not convolved with the band-power window function.

scanning strategy (see Fig. 7). The cosmology was that described in Sec. 1 (with reionization at  $z = 6$ ). The pseudo- $C_l$ s were extracted with HEALPix at resolution  $N_{\text{side}} = 512$  using the weight function shown in Fig. 7. This corresponds to inverse noise variance weighting for white noise in the time domain, and the azimuthal symmetry reflects the symmetry of the proposed BICEP scan strategy. We generated a further suite of Monte-Carlo noise realisations which were used to remove the noise bias. The integral in equation (90) was performed with a cumulative Simpson rule, giving estimates of  $\xi(\beta)$  at the roots of a Legendre polynomial scaled to the angular range  $(0, 31^\circ)$ . In principle we can estimate the correlation functions in the range  $(0, 37^\circ)$ , but very few pixel pairs contribute to the largest separation angles so the correlation functions are very noisy there. During the integration to form  $\xi(\beta)$  we constructed  $\xi_+(\beta)$  directly from the pseudo- $C_l$ s, with the noise bias removed, at points linearly spaced between the Legendre roots. (We used a nine-point Simpson rule.)

We recovered the angular power spectra by evaluat-

ing equation (85) with Gauss-Legendre quadrature. We adopted a Gaussian apodizing function with half-width at half-maximum equal to  $18^\circ.5$ . We further compressed our estimates into flat band-powers with a  $\Delta l = 35$  thus removing much of the sensitivity to the choice of apodization. We verified with Monte-Carlo simulations that  $\Delta l = 35$  is sufficient to remove any significant correlations between adjacent band powers. The mean band-powers for  $C_l^E$  and  $C_l^B$  (smoothed with the  $1^\circ$  beam) from 100 simulations are plotted in Fig. 8, along with  $\pm\sigma$  error boxes estimated from the simulations. From the simulations we have verified that the method is unbiased (to within the standard error of the Monte-Carlo averages). We also compared the errors estimated from the 100 simulations with the rule of thumb in equation (55). We found that to get good agreement with the Monte-Carlo errors on  $C_l^E$  it was necessary to refine equation (55) to take account of the noise inhomogeneity and the compression to band powers more properly. We used the following approximation to the covariance of the recovered beam-smoothed  $C_l^E$ s (see Efstathiou 2003 for a derivation of this formula for

the temperature anisotropies):

$$\begin{aligned} \text{cov}(\hat{C}_l^E, \hat{C}_{l'}^E) &\approx \frac{1}{2\pi(w_2 f_{\text{sky}})^2} \sum_L \left[ C_l^E C_{l'}^E \sum_M |(w_P^2)_{LM}|^2 \right. \\ &+ 2\sqrt{C_l^E C_{l'}^E} \sum_M (w_P^2 \sigma_P^2)_{LM} (w_P^2)_{LM}^* \\ &+ \left. \sum_M |(w_P^2 \sigma_P^2)_{LM}|^2 \right] \begin{pmatrix} l & l' & L \\ 0 & 0 & 0 \end{pmatrix}^2. \end{aligned} \quad (92)$$

Here,  $\sigma_P^2(\hat{\mathbf{n}})$  is the polarization noise variance per solid angle (see equation 47),  $w_P(\hat{\mathbf{n}})$  is the polarization weight function, and e.g.  $(w_P^2 \sigma_P^2)_{LM}$  are the (spin-0) multipoles of the product  $w_P^2(\hat{\mathbf{n}})\sigma_P^2(\hat{\mathbf{n}})$ . Equation (92) makes a number of approximations: (i) it takes no account of the need to separate  $E$  and  $B$ , which is reasonable for  $E$  given that it dominates  $B$ , but will not be valid if extended to  $B$  when  $C_l^E/C_l^B > (l\Delta_w)^2$ , where  $\Delta_w$  is the characteristic width of  $w_{P,l}$ ; (ii) it ignores the spin-2 nature of the polarization, which is acceptable at high  $l$ ; and (iii) it only treats the inversion from pseudo- $C_{ls}$  to  $\hat{C}_l$ s approximately (i.e. divide by  $w_2 f_{\text{sky}}$ ). We defer a full discussion of analytic approximations to the covariance of polarization power spectra to a future paper (Challinor & Chon in preparation), where we show how to generalise equation (92) to take account of  $E$ - $B$  mixing on an apodized sky. Here, we simply note that the above assumptions should hold well for  $C_l^E$  in this application to BICEP. For the level of  $C_l^B$  in our assumed cosmology ( $r = 0.31$ ), and given the smooth apodization of the edges of the survey region by  $w_P(\hat{\mathbf{n}})$ , the application of equation (92) to  $B$  should serve as a useful first approximation to the errors. Note also that, for uniform noise, we recover equation (55) if we average into bands that are wide compared to the power spectrum of the square of the weight function,  $\sum_m |(w_P^2)_{lm}|^2 / (2l+1)$ . The theoretical approximation to the errors in Fig. 8 are obtained by summing equation (92) over  $l$  and  $l'$  in a given band. These theoretical predictions agree well with the Monte-Carlo errors for  $E$ , and are in broad agreement for  $B$ . As expected, in the latter case the details of the  $E$ - $B$  separation process that are ignored in our rough theoretical predictions are more critical.

Our new estimator removes the cross-contamination between  $E$  and  $B$  in the mean, however, the variance of an estimate of  $C_l^E$  or  $C_l^B$  contains a contribution from both  $E$  and  $B$  modes. To assess more carefully the level of cross-contamination due to the geometric effect of  $E$ - $B$  mixing, we compute exactly the covariance of our decoupled power spectrum estimates in the absence of noise. Since the cross-contamination will be more significant for  $B$  than  $E$ , we concentrate on the former. We compute the error covariances first with  $E$  and  $B$  power retained, and then with only the  $B$  power. The latter calculation approximates the errors we would obtain if we separated the  $E$  and  $B$  modes at the level of the map prior to power spectrum estimation. The mechanics of the calculation are as follows. First, we compute the covariance of the polarization pseudo- $C_{ls}$  using the techniques described by Hansen & Górski (2003). This is only tractable because of the azimuthal symmetry of the BICEP scanning strategy. We then linearly transform the pseudo- $C_l$  covariance to that of the decoupled estimates using the fact that our power spectrum estimation method is linear in the pseudo- $C_{ls}$ , i.e.

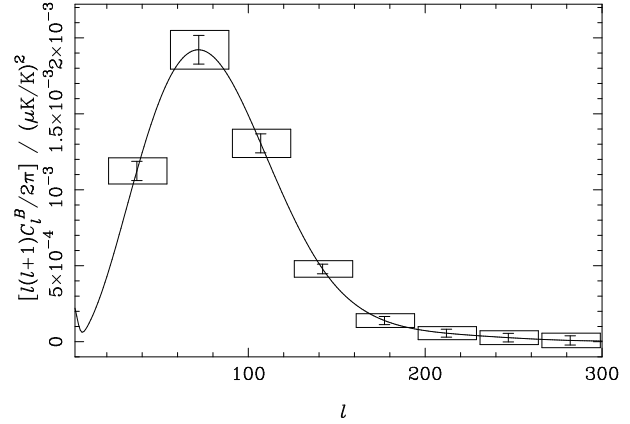


**Figure 9.** The variance of an estimate of  $C_l^B$  obtained by equation (93) in the absence of noise with the BICEP sky coverage. The boxes are the full error, including the cross-contribution from  $E$  modes. The bars are the variance obtained by setting  $C_l^E$  to zero, and thus are representative of the errors that would be achieved if  $B$  were separated from  $E$  at the level of the map.

$$\text{cov}(\hat{C}_l^X, \hat{C}_{l'}^{Y'}) = \sum_{L, L', X', Y'} M_{lL}^{XX'} \text{cov}(\tilde{C}_L^{X'}, \tilde{C}_{L'}^{Y'}) M_{l'L'}^{YY'}, \quad (93)$$

where  $X, X', Y$  and  $Y'$  run over  $E$  and  $B$ , and the coupling matrices relate the decoupled power spectrum estimates to the pseudo- $C_{ls}$ :

$$\hat{C}_l^X = \sum_{l'X'} M_{ll'}^{XX'} \tilde{C}_{l'}^{X'}. \quad (94)$$

The columns of the coupling matrices  $M_{ll'}^{XX'}$  are conveniently extracted by setting all of the pseudo- $C_{ls}$  to zero except for  $\tilde{C}_{l'}^{X'}$  in our power spectrum code, and then reading out the recovered  $\hat{C}_l^X$ . The matrix is symmetric on the indices  $X$  and  $X'$ . Figure 9 summarises our results obtained for the  $B$ -mode power spectrum. As in Fig. 8 we compress our results into flat band-powers. We see that, in the noise-free case, the errors we obtain using the BICEP weight function  $w_P(\hat{\mathbf{n}})$  are not dominated by the cross-contribution from  $E$ -mode polarization; this accounts for approximately only 20-per cent of the error budget. Of course, a lower level of  $B$ -mode polarization would increase the relative significance of the cross-contribution. Ultimately, this cross-contamination may make our method unsuitable for future, high-sensitivity  $B$ -mode experiments surveying small regions if the tensor amplitude is too low. We leave quantification of this statement to a future paper (Challinor & Chon in preparation), where we show how to estimate the cross-contribution to the variance for non-symmetric weight functions.

Since full covariance information is available from equation (93), the level of correlation between adjacent band-powers can be calculated directly. For the BICEP scan strategy,  $M_{ll'}^{XX'}$  oscillates with a full-width at half-maximum of approximately 12. Hence, for the chosen bin width  $\Delta l = 35$ , the correlation between adjacent bins is negligible.

## 6 CONCLUSION

We presented a fast and unbiased method to extract CMB polarization power spectra from large maps via the two-

point correlation functions. The method, which generalises that of Szapudi et al. (2001) to polarization, can be summarised as follows. First, we compute unbiased estimates of the three (complex) polarization auto- and cross-correlation functions at the roots of a Legendre polynomial from pseudo- $C_l$ s of heuristically-weighted maps. The estimates of the correlation functions can be computed in  $O(N_{\text{pix}}^{3/2})$  operations using fast spherical transforms. If the correlation functions can be estimated for all angular separations, the power spectra can be accurately recovered with Gauss-Legendre integration. In this case, the method is unbiased: the theoretical window function is a Kronecker delta. Further compression to band-powers can then be made, and the resulting theoretical window functions would be top-hat functions. If the correlation functions cannot be estimated for all angular separations, due to limitations of sky coverage, we showed that significant  $E$ - $B$  mixing can occur. In particular, large-scale  $E$  power (due to reionization) can be aliased into  $B$  on all scales. Although  $E$ - $B$  mixing does not present a fundamental problem for parameter extraction, it does complicate the interpretation (and presentation) of the recovered power spectra. For this reason, we proposed a new estimator, extending earlier work by Crittenden et al. (2002), that removes  $E$ - $B$  mixing exactly in the mean when working with incomplete correlation functions. Note that this is not the case for regularised inversions of the pseudo- $C_l$ s in harmonic space (e.g. by working with pseudo band powers as in a polarized extension of MASTER; Hivon et al. 2002). The new estimator requires one further numerical integration of the estimated correlation function  $\hat{\xi}_+(\psi)$  to obtain functions that contain only  $E$  or  $B$  power in the mean. Using e.g. a cumulative Simpson rule, these functions can be estimated accurately at the roots of a Legendre polynomial and inverted to power spectra with Gauss-Legendre quadrature. The increase in computational effort is minimal, and the theoretical window functions that result do not couple  $E$  and  $B$  power in the mean by construction. Fourier ringing in the estimates can be safely controlled by apodizing the integral transforms (or by compressing into band-powers), without introducing any  $E$ - $B$  mixing.

An essential part of our method (and indeed any quadratic method) is being able to remove the mean noise contribution from the correlation functions (i.e. to remove the bias due to the noise). For general noise properties we must resort to Monte-Carlo evaluation of the mean over an ensemble of pure noise realisations. The method presented here is thus dependent on being able to simulate noise maps efficiently. Error estimation on the recovered  $C_l$ s must also generally proceed by Monte-Carlo evaluation. The  $O(N_{\text{pix}}^{3/2})$  scaling of our method makes this a realistic proposition, even for mega-pixel maps.

We applied our methods to simulations of a large-area survey, with parameters similar to *Planck*, and also to the BICEP experiment which will cover 3 per cent of the sky. In both cases we obtained errors in line with theoretical expectations. Although our algorithm in its present form is already practical for analysing mega-pixel CMB maps, further work is required to assess the optimality of the underlying methods. In particular, comparison with current (brute-force) maximum-likelihood codes should be possible for low-resolution simulations; comparison at higher resolution must await further algorithmic development of the

likelihood codes. Another issue worth investigating further is the impact of the choice of pixel weighting on the cosmic variance contribution from e.g.  $C_l^E$  to the recovered  $C_l^B$ . Although we have separated  $E$  and  $B$  in the mean, this does not guarantee that in a single realisation there is no recovered  $B$  power due to  $E$  modes in the signal. We have shown that this geometric effect does not dominate the error budget for  $C_l^B$  for the BICEP weight function, in the absence of noise, for a tensor-to-scalar ratio of  $r = 0.31$ . However, ultimately this cross-contribution may limit the applicability of our method if the tensor amplitude is low enough (Challinor & Chon in preparation). To eliminate this undesirable contribution to the variance would require separating  $E$  and  $B$  at the level of the map, e.g. Lewis et al. (2002), prior to performing power spectrum estimation.

## ACKNOWLEDGEMENTS

We thank Robert Crittenden for useful discussions at the start of this project, Antony Lewis for help with the integrals in the Appendix, and Stephane Colombi for help with issues of implementation. ADC acknowledges a Royal Society University Research Fellowship, and IS was supported by NASA through AISR grants NAG5-10750, NAG5-11996, and ATP grant NASA NAG5-12101 as well as by NSF AST02-06243. Some of the results in this paper have been derived using the HEALPix (Górski, Hivon & Wandelt 1999) package.

## REFERENCES

- Benabed K., Bernardeau F., van Waerbeke L., 2001, *Phys. Rev. D*, 63, 043501
- Bond J. R., Jaffe A. H., Knox L., 1998, *Phys. Rev. D*, 57, 2117
- Bunn E. F., 2002, *Phys. Rev. D*, 65, 043003
- Bunn E. F., Zaldarriaga M., Tegmark M., de Oliveira-Costa A., 2003, *Phys. Rev. D*, 67, 023501
- Chiueh T., Ma C.-J., 2002, *ApJ*, 578, 12
- Crittenden R. G., Turok N. G., 1998, preprint (astro-ph/9806374)
- Crittenden R. G., Natarajan P., Pen U.-L., Theuns T., 2002, *ApJ*, 568, 20
- Efstathiou G., 2003, preprint (astro-ph/0307515)
- Górski K. M., Hivon E., Wandelt B. D., 1999, in Banday A. J., Sheth R. S., Da Costa L., eds, *Proceedings of the MPA/ESO Cosmology Conference "Evolution of Large-Scale Structure"*, PrintPartners Ipskamp, NL, p. 37
- Hansen F. K., Górski K. M., 2003, *MNRAS*, 343, 559
- Hansen F. K., Górski K. M., Hivon E., 2002, *MNRAS*, 336, 1304
- Hivon E., Górski K. M., Netterfield C. B., Crill B. P., Prunet S., Hansen F., 2002, *ApJ*, 567, 2
- Kamionkowski M., Kosowsky A., Stebbins A., 1997, *Phys. Rev. Lett.*, 78, 2058
- Kesden M., Cooray A., Kamionkowski M., 2002, *Phys. Rev. Lett.*, 89, 011304
- Kinney W. H., 1998, *Phys. Rev. D*, 58, 123506
- Kogut A. et al., 2003, *Astrophys. J. Suppl.*, 148, 161
- Kovac J., Leitch E. M., Pryke C., Carlstrom J. E., Halverson N. W., Holzappel W. L., 2002, *Nature*, 420, 772

- Lewis A., Challinor A., Turok N., 2002, *Phys. Rev. D*, 65, 023505
- Martin J., Schwarz D., 2000, *Phys. Rev. D*, 62, 103520
- Newman E., Penrose R., 1966, *J. Math. Phys.*, 863
- Ng K., Liu G., 1999, *Int. J. Mod. Phys. D*, 8, 61
- Oh S. P., Spergel D. N., Hinshaw G., 1999, *ApJ*, 510, 551
- Sbarra C., Carretti E., Cortiglioni S., Zannoni M., Fabbri R., Macculi C., Tucci M., 2003, *Astron. Astrophys.* 401, 1215
- Seljak U., Zaldarriaga M., 1997, *Phys. Rev. Lett.*, 78, 2054
- Szapudi I., Prunet S., Colombi S., 2001, *ApJ*, 561, L11
- Tegmark M., de Oliveira-Costa A., 2002, *Phys. Rev. D*, 64, 063001
- Varshalovich D. A., Moskalev A. N., Khersonskii V. K., 1988, *Quantum Theory of Angular Momentum*. World Scientific, Singapore
- Wandelt B. D., Hansen F. K., 2003, *Phys. Rev. D*, 67, 023001
- Wandelt B. D., Hivon E., Górski K. M., 2001, *Phys. Rev. D*, 64, 083003
- Zaldarriaga M., 1997, *Phys. Rev. D*, 55, 1822
- Zaldarriaga M., 2001, *Phys. Rev. D*, 64, 103001
- Zaldarriaga M., Seljak U., 1998, *Phys. Rev. D*, 58, 023003

## APPENDIX A: $A(\psi)$ FOR UNIFORMLY-WEIGHTED, AZIMUTHALLY-SYMMETRIC PATCHES

In the special case that the analysis is performed over an azimuthally-symmetric part of the sky with uniform pixel weighting  $w(\hat{\mathbf{n}}) = 1$ , the correlation function normalisation  $A(\psi)$  can be evaluated analytically. (We can drop the subscripts  $P$ ,  $T$  and  $X$  in this case since there is no distinction between the normalisations.)

We begin by considering a polar-cap region with angular radius  $\alpha$ , and assume that  $\alpha \leq \pi/2$ . The integral in equation (31) then evaluates to give

$$\frac{1}{A(\psi)} = 4\pi \left[ \cos^{-1} \left( \frac{2 \sin^2(\psi/2)}{\sin^2 \alpha} - 1 \right) - \cos \alpha \cos^{-1} \left( \frac{2 \tan^2(\psi/2)}{\tan^2 \alpha} - 1 \right) \right] \quad (\text{A1})$$

for  $\psi \leq 2\alpha$ , and zero otherwise. Note that  $1/A(0) = 4\pi^2(1 - \cos \alpha) = 8\pi^2 f_{\text{sky}}$  as required by equation (53). Note also that  $1/A(\psi)$  goes continuously to zero as  $\psi \rightarrow 2\alpha$ . We can now construct the other important case of a Galactic cut by symmetry. For a symmetric cut subtending an angle  $\alpha_c$ , provided that  $\alpha_c \leq \pi/2$ , there are pixel pairs at all angular separations and  $1/A(\psi)$  is non-zero for all  $\psi \in (0, \pi)$ . If we denote the normalisation for a polar-cap region of angular radius  $(\pi - \alpha_c)/2$  by  $A_*(\psi)$ , then we find

$$\frac{1}{A(\psi)} = \begin{cases} \frac{2}{A_*(\psi)} & 0 \leq \psi \leq \alpha_c, \\ \frac{A_*(\psi)}{A_*(\psi)} + \frac{2}{A_*(\pi-\psi)} & \alpha_c \leq \psi \leq \pi - \alpha_c, \\ \frac{2}{A_*(\pi-\psi)} & \pi - \alpha_c \leq \psi \leq \pi. \end{cases} \quad (\text{A2})$$

This paper has been typeset from a  $\text{\TeX}/\text{\LaTeX}$  file prepared by the author.